TENTH AUSTRALASIAN FLUID MECHANICS
CONFERENCE - UNIVERSITY OF MELBOURNE
11-15 DECEMBER 1989

NUMERICAL STUDY FOR THE SHEDDING OF VORTICITY FROM A SEMI-INFINITE PLATE

YU, Ching-Fu and SOH, Wee-King

Department of Mechanical Engineering
University of Wollongong
P.O. Box 1144, Wollongong NSW 2500
AUSTRALIA

Abstract - This paper is concerned with the shedding of vorticity from a semi-infinite plate which is parallel to the free stream. The flow separation from the right-angled corners of the leading edges is computed by using a vortex sheet technique. The computed free shear layer, which rolls up into a large spiral, is found to contain secondary spirals termed as small-scale spirals. The behaviour of these small-scale spirals and other flow phenomena are investigated from the results of three cases of unsteady flow: (i) flow in steady free stream velocity; (ii) flow perturbed by resonance frequency; and (iii) flow with forced perturbation.

1. Introduction

Flow in the separated and reattached regions along a body is characterized by a separation bubble just between the separation point and the point of reattachment. This kind of flow has been recognized to be very important in engineering. There have been many investigation of a wide variety of flow configurations. Examples include the air around the heated steel plate which has just moved out from the rolling mill; the flow around a solar collector and the flow around roughness elements of various shapes attached to a surface, such as the fins of a heater exchanger and the blades of a gas turbine. The vortex which is generated by the flow separation, has a strong perturbing effect on the boundary-layer structure and consequently it plays a significant role in fluid engineering systems.

In order to investigate the problem of two-dimensional vortex shedding around a cylinder of rectangular shape, earlier researchers (Clements (1973); Sarpkaya (1975); Kiya, Sasaki & Arie (1982); Nagano, Natto & Takata (1982)) approximated the free shear layer by a discrete-vortex model and predicted the dominant feature of the flow. Furthermore, Thompson & Hourigan (1986) combined finite-difference and discrete-vortex techniques to investigate an acoustically perturbed two-dimensional separated flow around a heated plate and predicted a number of features concerning to the separation flow and the heat transfer coefficient.

The above discrete vortex methods, with a variety of numerical approaches, give steady state results which are in good agreements with experiments. The aim of this work is to investigate the mode of transient flow in the area between the points of flow separation and reattachment with the vortex sheet method suggested by Soh, Hourigan & Thompson (1988).

2. Mathematical description of the model

Consider a semi-infinite plate with finite thickness and square leading edge which is aligned parallel to a uniform approaching stream. The shear layers shed from the front corners of the plate are approximated by arrays of vortex sheet elements. The motion of the shear layers is represented by the evolution of these elements in time. The velocities of a vortex sheet element consists of a component from the two-dimensional irrotational potential flow around the plate and a component which is induced by the all vortex sheet elements. These velocities can be calculated with the help of the Schwarz-Christoffel transformation.

2.1 Schwarz-Christoffel transformation

In the physical plane, there is a semi-infinite plate of thickness 2h which extends to infinity along the positive real axis. By using the Schwarz-Christoffel transformation, the region outside of the semi-infinite plate in the physical plane (z-plane) can be mapped onto the upper half of the transformed plane (λ-plane) as represented by equation (1). The corners on the plate B and C, at $z=\pm ih$, are mapped into $\lambda=\pm 1$, respectively.

$$z = \frac{2hi}{\pi}\left[\sin^{-1}(\lambda) + \lambda(1-\lambda^2)^{1/2}\right] \quad (1)$$

2.2 Discretization of a vortex sheet

Computations are carried out in the transformed plane (λ-plane). The image of the vortex sheet, in the λ-plane, is discretized into N number of small straight vortex sheet elements such that the jth element has a vorticity γ_j distributed over its length Δs_j. The other parameters associated with each element are: the angle of inclination with the real axis, θ_j, and the pivotal point being the mid-point of the element - denoted λ_j, which is z_j in the physical plane. The flow separation from the right-angled corners of the leading edges is computed by applying the Kutta condition to the separated shear layer, which is represented by a vortex sheet. The vorticity density γ_j is assumed to be uniformly distributed in each element.

2.3 The velocity

The configuration of the flow consists of a free stream and a vortex sheet attached to the leading corner B of the plate. The free stream has a magnitude of U_0 and is parallel to the real axis. The complex velocity for a point λ_i which has a complex potential, ω, is given by

$$u(\lambda_i) - iv(\lambda_i) = \frac{d\omega(\lambda_i)}{d\lambda}\left|\frac{d\lambda}{dz}\right|^2_{\lambda_i} \quad (2)$$

with

$$\left.\frac{d\lambda}{dz}\right|_{\lambda_i} = -\frac{i\pi}{4h}\frac{1}{(1-\lambda_i^2)^{1/2}} \quad (3)$$

and

$$\frac{d\omega(\lambda_i)}{d\lambda} = \frac{4hU_0\lambda_i}{\pi} +$$

$$\sum_{I=1}^{4}\left[\frac{1}{2\pi i}\sum_{j=1}^{N}\int_{-\Delta s_{j-1/2}}^{\Delta s_{j+1/2}}\frac{\gamma_j(s)\, ds_{\lambda_j}}{\lambda_i-\lambda_j-s\,e^{i\theta_j}}\right]_I \tag{4}$$

The integration is along the length of the elements, s, with local origin on each pivotal point. The limits of the integration $\Delta s_{j+1/2}$ and $\Delta s_{j-1/2}$, are the distances between the pivotal point and the edges of the element, so that the jth element has a length of $\Delta s_j = \Delta s_{j+1/2} + \Delta s_{j-1/2}$. Subscript I represents the vortex sheet in the first quadrant of the transformed plane and the appropriate images in the second, third, and fourth quadrants.

2.4 Determination of the initial distribution of vorticity

The vortex sheet method, unlike point vortex method which usually starts with one vortex, needs to begin with an array of elements. It becomes necessary to prescribe the shape and distribution of an initial vortex sheet just to initiate the computation.

A short vertical vortex sheet with one end attached to the separation point, a corner of the plate, is considered. The distribution of vorticity density is given by

$$\gamma^*(s^*) = 2Ks^*\,(1 - s^{*2})^{-1/2} \tag{5}$$

where s* is the distance of the vortex element from the separation point and γ^* is the given strength of vortex elements. Since the Kutta condition requires that the flow in the λ-plane is stagnation at $\lambda = \pm 1$, this is expressed as

$$\frac{d\omega}{d\lambda} = 0 \qquad \text{at } \lambda = \pm 1 \tag{6}$$

Equation (6) can be satisfied by an appropriate value for K and this determines the function $\gamma^*(s^*)$ in equation (5).

2.5 The Kutta condition: calculation of the generated circulation from a corner

Two methods have often been used in the vortex methods for determining the strength of a nascent vortex and its position. In one method, the nascent vortex is placed at a certain fixed point and its strength is determined by satisfying the Kutta condition. In the other, the strength of the nascent vortex is determined by a simplified concept of boundary layer theory and its position is found by satisfying the Kutta condition.

Clements (1973) considered that the velocity at separation points would be zero to satisfy the no-slip condition. Hence the vortex which leaves the separation point is determined by the velocity U'_s at the outer edge of the boundary layer. The rate of vorticity shedding into the shear layers is determined by the relationship $d\Gamma'/dt = 0.5U'^2_s$. On the other hand, Sarpkaya (1975) stated that the rate at which vorticity is shed into the wake is given by

$$\int_0^{\delta}\left[\frac{\partial v}{\partial x} - \frac{\partial u}{\partial y}\right] u\, dy \tag{7}$$

where δ is the boundary-layer thickness. This may be closely approximated by

$$\frac{\partial\Gamma}{\partial t} = \frac{1}{2}\left(V_1^2 - V_2^2\right) \simeq \frac{1}{2}V_1^2 \tag{8}$$

where V_1 and V_2 represent the velocities at the outer and inner edges of the shear layer. He introduced a 'nascent vortices', also called 'Kutta vortices', near the edge of the plate so that at the start of each time step the Kutta condition is satisfied at the edge.

The present method uses the concept stated in equation (7). Writing VIN as the numerical approximation of V_1 in equation (8), and GN as the circulation in the nascent element, the result is

$$GN = -\frac{1}{2}\, VIN^2\, \Delta t \tag{9}$$

The negative sign is related to the direction of the generated circulation which is positive for counter-clockwise and Δt is the time increment. The no-slip condition is satisfied exactly only at the instant of the introduction of each new vortex. It ceases to be valid during the remainder of the time step by the very nature of discretization.

2.6 Outline of computation

The computational steps are summarized as followings:
1) Initially a straight vortex sheet, consists of 10 elements with Δs equals to 0.01, is placed at 60° to the real axis for the λ-plane. The vorticity distribution is given by equation (5).
2) The velocity VIN is the image velocity in the λ-plane at λ=1. It is calculated from equation (2) and resulted in the formula: $VIN = |d\omega(\lambda)/d\lambda|.|d\lambda/dz|^2$. The time step is calculated by the formula: $\Delta t = \Delta s/VIN$.
3) The pivotal points in the λ-plane is displaced to a new position over a time step Δt, by the Euler integration formula: $\lambda_j(t+\Delta t) = \lambda_j(t) + (u_j(\lambda)dt - iv_j(\lambda))\Delta t$. The edges of each element are transported in the same manner except that their velocities take the form of the average between the two adjacent pivotal points. The edge of the element at the free end of the vortex sheet moves with the pivotal point of the element.
4) The circulation , ΔΓ, of the nascent vortex element is $\Delta\Gamma = -0.5VIN^2\,\Delta t$.
5) The process of rediscretization as given by Fink & Soh (1978), which readjusts all elements into equal length, is used once per 10 time steps.
6) A new element of length Δs is generated from the separation point and becomes part of the vortex sheet.
7) The steps from (2) to (6) are repeated as many times as needed.

3. Results and discussion

The flow is symmetrical about the real axis. Normalization of parameters is achieved by setting h and U_0 to unity.

3.1 Case 1: Flow in constant free stream velocity

Figures 1 (a)~(b) show the situations of rolled-up vortex sheet around the plate in the flow of constant free stream velocity for t=2.356 and 2.701. The length of the element is 0.015 and the number of element, NE, are 447 and 614, respectively. It is evident that the vortex sheet is rolling up into a large spiral. The free end of the vortex sheet is found outside of the spiral. There are a few small-scale rolled-up structures, small separation bubbles, within the large spiral. The number of these small-scale spirals continue to increase with time. The amalgamation between adjacent small-scale spirals can be observed in these figures.

Amsden & Harlow (1964) explained these results in term of "slip instability" in the flow. These small scale spirals also represent local concentration of vorticities as reported by Nagata et al. (1985). In their experimental observation, Nagata et al. claimed that the turbulence in the vortex region is caused by the centrifugal instability owing to the local concentration of vorticity. The larger amount of vorticity shed from the secondary vortex will give rise to a larger concentration of vorticity which causes the shear layer to undulate and roll up locally. It is suggested that this local undulation in the free shear layer is related to the transition to turbulent flow.

The penetration problem mentioned by Kuwahara (1973) does not appear in the present results. From the diagrams of roll-up vortex sheet in figures 1 (a)~(b), the vortex sheet, which becomes a large rolled-up spiral structure, does not penetrate the surface of the plate. There is a region next to the free end of the vortex sheet which evolves and comes very close to the surface of the plate. The distance between the vortex sheet and the surface of the plate is about 0.02.

3.2 Case 2: Flow with perturbed shedding of vorticity

A perturbation is achieved by introducing a sinusoidal component. Thus, the circulation of the nascent vortex element, GN^*, is given by

$$GN^* = GN\ (1 + A \sin 2\pi ft) \qquad (10)$$

where

$GN = 0.5\ (VIN)^2\ \Delta t$, is the result of Kutta condition, see equation (9)
VIN = The velocity of the nascent vortex element
Δt = Time step
A = The amplitude of the oscillation
f = The frequency of the oscillation
t = Time

Figures 2 shows the evolution of the vortex sheet near the upper corner of the plate at t=1.895. These results are derived from f=0.07, A=0.1 and Δs=0.02. The corresponding Strouhal number is 0.14. It lies in the middle of the resonance ranges of 0.1 to 0.12 and 0.18 to 0.21 which are discovered by Parker & Welsh (1983). The formation of numerous small spirals throughout the whole of the roll-up vortex sheet is a reminiscence of the observations by Prandtl (1904) and the spark shadowgraph by Pierce (1961), the computed results by Hama (1962). Pullin & Perry (1980) regard the appearance of these patterns is essentially caused by the unstable nature of the free shear layer as well as the interference by an apparatus. In the investigation of a starting flow behind a triangular prism in uniform and stratified flow, Huhe et al. (1983) observed small spirals within the roll-up vortex sheet and stated that the vibrations of the apparatus was the cause of this instability.

Kelvin-Helmholtz instabilities in the vortex sheet will lead to the formation of small-scale spirals as shown in case 1. Any perturbations at resonance frequency, such as in this case, will enhance the structure of these small-scale spirals. In the perturbed shedding of vorticity, the spacing between adjacent small-scale spirals increases with respect the arc length from the point of flow separation.

The movements of these small-scale spirals can be presented by plotting the arc length of the spiral from the point of flow separation against the index of the spiral. The index is an integer which identifies the spiral. An index of 1 represents the spiral nearest to the point of flow separation. The plots for various time, as shown in figure 3, are normalized by scaling such that the arc length to the first spiral becomes a unity. These curves form an envelop which is the steady state line. It is interesting to note that the plot for Pierce's spirals fall on this envelop. This plot of spiral index is a convenient way for comparing the patterns of small-scale spirals from different sources.

A check on the core of the roll-up large spiral shows that it travels at a velocity $0.59U_0$. Although this is 18% higher than $0.5U_0$ which was measured by Pierce in the shedding of free shear layer from the edge of a plate in the impulse motion, it is still within the range (0.5-0.6) U_0 reported by Kiya (1986).

3.3 Case 3: Flow with small oscillation in the free stream

A perturbation component is introduced into the free stream, U^*, as shown in equation (11).

$$U^* = U_0\ (1 + A \sin 2\pi ft) \qquad (11)$$

where U_0 is the mean velocity and is set to unity. Figure 4 shows the results for A=0.1, f=0.24 and Δs=0.02. The corresponding Strouhal number is 0.48 which is outside the resonance range. The forced oscillation has generated small-scale spirals. However, unlike the small-scale spirals in case 2, they only survive for a short time before being engulfed by the large roll-up vortex sheet spiral. Only four small-scale spirals can be maintained as shown in figure 4. The overall structure of the large vortex sheet spiral seems to be unaffected by Strouhal number. The core is found to travel at a velocity of $0.60U_0$ as compares with $0.59\ U_0$ in case 2.

4. Concluding remarks

The shedding of vorticity over a semi-infinite plate have been numerically studied by using a vortex sheet technique. This includes three cases of unsteady flow: (i) flow in constant free stream velocity, (ii) flow with perturbed shedding of vorticity at resonance frequency, and (iii) flow with forced oscillation of the free stream.

Unlike vortex sheet from an elliptical loaded wing which has a strong tendency to roll up, Fink & Soh (1978), the present flow system restricts a vortex sheet to a region near the surface of a plate and this restriction gives rise to a slower rolling up motion. The consequence is the formation of small-scale spirals within the large roll-up vortex sheet. These structure of small-scale spirals, which are suspected to be caused by Kelvin-Helmholtz's instability, become very prominent when the flow is perturbed under resonance frequency. Forced periodical perturbation may also give rise to these small-scale spirals but they soon disappear into the large roll-up vortex sheet.

A calculation using the perturbation as in case 2 but with a Strouhal number equals 0.48, shows results very similar to that of case 3. It can be concluded that the frequency of the perturbation is by far more influential to the mode of flow separation than its sources. This has been been demonstrated by Stokes, Welsh & Hourigan (1986) in their simulation of acoustic excitation using the correct frequency but with a different source of excitation.

The size of the separation bubble can be examined by plotting Xr, the distance of the stagnation point from the point of flow separation, against time, t, as shown in figure 5. It is evident that the loci of the stagnation points for all three cases are identical and, with the exception of near starting time, all fall into a straight line given by

$$Xr = 0.224 + 0.966\ t \qquad (12)$$

This indicates that the initial growth rate of the separation bubble is constant, 0.966U, and is also independent of the Strouhal number.

Numerical accuracy is important for these results. The size of the element, Δs, should be less than 0.05 in order to give a reasonable resolution for the simulation of small-scale spirals. Results shown here are calculated by using Δs in the range from 0.01 to 0.03.

It is found that the movement of the vortex sheet is very small over the prescribed time step, Δt. In order not to inhibit the growth of the vortex sheet, it is necessary to make the errors caused by the rediscretization process to be at least an order smaller than the actual displacement of the vortex sheet. This requirement can be fulfilled by applying the rediscretization process once in every 10 time steps.

5. References

Amsden, A.A. and Harlow, F.H. (1964) Slip Instability. Physics of Fluids 7 (3), pp. 327-334 .

Clements, R. R. (1973) An Inviscid Model of Two-Dimensional Vortex Shedding. Journal of Fluid Mechanics

57 (2), pp. 321-336 .

Fink, P. T. and Soh, W. K. (1978) A New Approach to Roll-up Calculations of Vortex Sheets. Proc. Roy . Soc. Lond. A. 362, pp.195-209.

Hama, F.R. (1962) Streaklines in a Perturbed Shear Flow. Phys. Fluids 5, pp. 644-650 .

Huhe, A., Yan M., Zhang, B. and Liu , K. (1983) Experimental Study of Starting Flow behind A Triangular Prism in Uniform and Stratified Flow. Proceedings of the Second Asian Congress of Fluid Mechanics, Beijing, China, pp. 807-812 .

Kiya, M. (1986) Structure of Flow in Leading-edge Separation Bubbles. Smith, F.T. & Brown, S.N. (Eds.), Boundary-Layer Separation, IUTAM Symposium, London, pp. 57-71 .

Kiya, M., Sasaki, K., and Arie, M. (1982) Discrete Vortex Simulation of A Turbulent Separation Bubble. Journal of Fluid Mechanics 120, pp. 219-244.

Kuwahara, K. (1973) Numerical Study of Flow past an Inclined Flat Plate by an Inviscid Model. Journal of The Physical Society of Japan 35 (5), pp. 1545-1551 .

Nagano, S., Natto, M. and Takata, H. (1982) A Numerical Analysis of Two-Dimensional Flow Past a Rectangular Prism by a Discrete Vortex Model. Computer and Fluids 10 (4), pp. 243-259.

Nagata, H., Funada, H., Kawai, K. and Matsui, T. (1985) Unsteady Flows in the Vortex Region Behind a Circular Cylinder Started Impulsively. Bulletin of JSME 28 (245), pp. 2599-2607 .

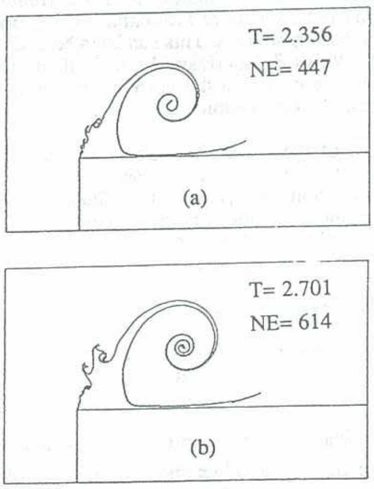

Figure 1 The evolution of the vortex sheet around a semi-infinite plate in a constant free stream velocity. (a) t=2.356 and (b) t=2.701.

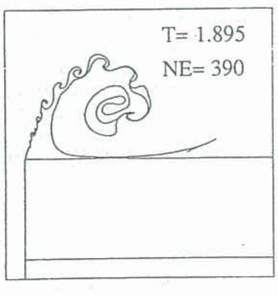

Figure 2 The evolution of the vortex sheet around a semi-infinite plate with perturbed shedding of vorticity at t=1.895.

Parker, R. and Welsh, M.C. (1983) Effects of Sound on Flow Separation from Blunt Flat Plates. Int. J. Heat & Fluid Flow. 4 (2), pp. 113-127.

Pierce, D. (1961) Photographic Evidence of the Formation and Growth of Vorticity behind Plates Accelerated from Rest in Still Air. Journal of Fluid Mechanics 11, pp. 460-464 .

Prandtl, L. (1904) Über Flüssigkeitsbewegung bei sehr kleiner Reibung. Verhandlungen des III. Internationalen Mathematiker-Kongresses, Heidelberg .

Pullin, D.I. and Perry, A.E. (1980) Some Flow Visualization Experiments on the Starting Vortex. Journal of Fluid Mechanics 97 (2), pp. 239-255.

Sarpkaya, T. (1975) An Inviscid Model of Two-Dimensional Vortex Shedding for Transient and Asymptotically Steady Separated Flow Over an Inclined Plate. Journal of Fluid Mechanics 68 (1), pp. 109-128 .

Soh, W.K., Hourigan, K. and Thompson, M.C. (1988) The Shedding of Vorticity from a Smooth Surface. Fluid Dynamics Research 3, pp. 122-126.

Stokes, A.N., Welsh, M.C. and Hourigan, K.(1986) Sound Generated by Separated Flows around Bluff Bodies. 9th Australasian Fluid Mechanics Conference, Auckland, pp.164-167

Thompson, M.C. and Hourigan, K. (1986) Combined Finite-Difference and Discrete-Vortex Solution of Acoustically Perturbed Two-Dimensional Separated Flow Around a Heated Plate. CTAC-85, pp. 405-416.

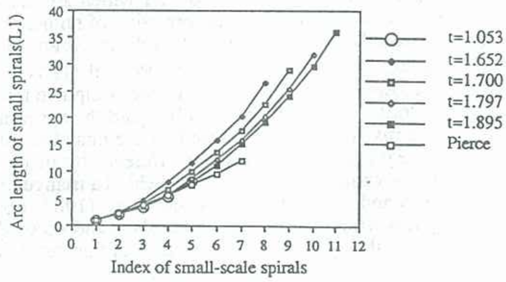

Figure 3 Plot of the arc-length of the small-scale spirals against their indices (smaller index represents spiral nearer to the point of flow separation).

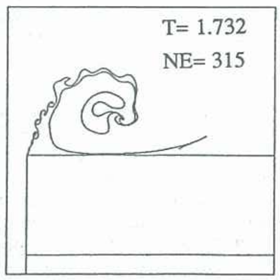

Figure 4 The evolution of the vortex sheet around a semi-infinite plate in the flow with small oscillation of the free stream at t=1.732.

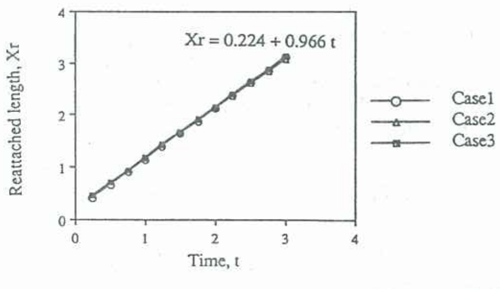

Figure 5 The relationship between the reattached length, Xr, and time, t.